ELECTRON AND HOLE MOBILITY IN SEMICONDUCTOR DEVICES

Carrier mobility in a semiconductor is one of the most important parameters for the operation of electronic devices. Actually, the mobility measures the ability of free carriers (electrons or holes) to move in the material as it is subjected to an external electric field. The magnitude of the mobility directly impacts on the device performance since it determines the operation speed through the transit time across the device, the circuit operating frequency, or the sensitivity in magnetic sensors.

Therefore, for a long time, the search for materials with the highest mobility has driven the research in the electronics industry. In practice, only two semiconductors, silicon (Si) and gallium arsenide (GaAs), have been recognized as being the most suitable for the viewpoint of industrial standards. Silicon is the leading semiconductor material for today's electronics since it is used in more than 95% of the semiconductor market. Silicon is mostly used for very large-scale integration (VLSI) microelectronics including bipolar and metal-oxide-semiconductor (MOS) transistors technologies which feature high complexity and large speed (microprocessor, microcontroller, microsystem, etc.) or large memory capacity [Static Random Access Memory (SRAM), Dynamic Random Access Memory (DRAM), Electrically Erasable Programmable Read-Only Memory (EEPROM), etc.]. GaAs is well suited for very

J. Webster (ed.), *Wiley Encyclopedia of Electrical and Electronics Engineering*.

high speed electronics with operating frequencies from 10 GHz to 100 GHz because of its higher mobility (as compared to silicon). GaAs is the leading material used in optoelectronic applications because of its direct optical bandgap which allows high photonic quantum yield.

The carrier mobility in a material is limited by various scattering mechanisms whose effect is to deviate the carrier trajectory or to absorb the energy gained by the carriers following the electric field acceleration. Typical scattering processes include lattice vibrations (phonons), charged impurities, crystal imperfections, interfaces or surfaces, and interactions with other carriers. It is intuitively obvious that the mobility will be larger in crystalline semiconductors with low density of defects, small number of phonons, and light carrier effective mass. The latter aspect is basically related to the band structure of the material and, in turn, cannot be easily improved by the fabrication process. The phonon number can significantly be attenuated by decreasing the lattice temperature, resulting in a higher mobility that justifies the low temperature operation as an effective means for circuit performance improvement. The quality of the raw material is not a concern due to the tremendous progress realized in crystal growth techniques, especially in the silicon industry where wafers as large as 30 cm with less than one defect per square centimeter are commercially available. As a result, the carrier mobility in the semiconductor substrate is essentially limited by the presence of intentional doping impurities in the active regions of the components such as the base of bipolar devices and the channel of field effect transistors (FET).

In this article the basic aspects of electronic transport in a semiconductor will be addressed, first with a special emphasis on the mobility behavior. Then a brief review of the transport properties for Silicon and GaAs will be presented owing to typical electron and hole mobility data for majority and minority carriers. Finally, some specific mobility results for field effect transistors such as Si MOSFETs and GaAS heterostructure field effect transistors (HFET) will be discussed. It should be mentioned that only the electronic transport under low electric condition will be treated in this article. Information about high field transport can be found elsewhere (see article on hot electron in semiconductor).

The favorable properties of silicon–germanium alloys have recently stimulated increasing activities in the area of device research. Tremendous performances for n–p–n heterojunction bipolar transistors and p-type MOSFETs have thus been obtained using SiGe base or SiGe buried channel. The mobility behavior in such material goes beyond the scope of this article. The interested reader can find appropriate information in the literature (1,2).

BASIC THEORY OF ELECTRONIC TRANSPORT IN SEMICONDUCTORS

As a carrier of charge q, say an electron, is accelerated by a low electric field $\mathbf{F}$, its instantaneous velocity is proportional to the time t as $\mathbf{v}(t) = qt\mathbf{F}/m^*$, with m^* being its effective mass. Indeed, if no scattering processes were present, it would reach an infinite speed. In steady-state regime, the drift velocity $\mathbf{v}$ of the carrier becomes saturated and is proportional to the mean time between two collisions τ such that,

$$\mathbf{v} = \frac{q\tau}{m^*}\mathbf{F} = \mu_c\mathbf{F} \tag{1}$$

The proportionality factor between the drift velocity and the electric field is by definition the carrier mobility μ_c. For an ensemble of carriers of volume density n, the resulting current is $\boldsymbol{J} = qn\mathbf{v}$, which allows the electrical conductivity to be defined as $\sigma = \mathbf{J}/\mathbf{F} = q\mu_c n$ (Ohm's law).

In the case of a semiconductor the carriers have a distributed kinetic energy E which has to be taken into account for real calculation of conductivity and mobility. The Boltzmann transport equation or the Kubo–Greenwood integral can in general be used to evaluate such quantities yielding the following important relations (3–6):

$$\sigma = \int_0^\infty \sigma(E)\left(-\frac{\partial f}{\partial E}\right)dE \quad \text{and}$$
$$\mu_c = \frac{\sigma}{qn} = \frac{\int_0^\infty \sigma(E)\left(-\frac{\partial f}{\partial E}\right)dE}{\int_0^\infty qN(E)f(E)\,dE} \tag{2}$$

where $\sigma(E) = 2qE\mu(E)N(E)/3$ is called the energy conductivity function: $\mu(E) = q\tau(E)/m^*$ is the energy mobility function related to the mean scattering time $\tau(E)$, for each energy E; $N(E)$ is the band density of states (mostly parabolic $\propto E^{1/2}$); and $f(E)$ is the Fermi–Dirac function. Actually, $\sigma(E)$ and $\mu(E)$ represent the conductivity and mobility, respectively, if the Fermi level E_f were placed at a given energy in the band. This situation occurs when degeneracy is reached: that is, for a highly doped semiconductor or a metal where the Fermi level lies in the conduction band.

In presence of a magnetic field $\mathbf{B}$ perpendicular to the applied electric field $\mathbf{F}$, the carriers are subjected to the Lorentz force $\mathbf{f} = q\mathbf{v} \times \mathbf{B}$, which is counterbalanced by an electrical force associated with the Hall electric field $\mathbf{F}_H = -\mathbf{f}/q = -R_H\mathbf{J} \times \mathbf{B}$ with $R_H \approx 1/(qn)$ being the Hall constant (see HALL EFFECT TRANSDUCERS). The Hall mobility is given by definition as $\mu_H = R_H\sigma$. It can be shown that in the Kubo–Greenwood formulation it is related to $\sigma(E)$ and $\mu(E)$ as (4,7),

$$\mu_c = \frac{\int_0^\infty \mu(E)\sigma(E)\left(-\frac{\partial f}{\partial E}\right)dE}{\int_0^\infty \sigma(E)\left(-\frac{\partial f}{\partial E}\right)dE} \tag{3}$$

The Hall mobility is therefore different from the conductivity mobility μ_c. The ratio $r = \mu_H/\mu_c$ is called the Hall factor and is close to unity in most cases (8). The detailed calculation of the mobility requires the specification of the scattering process energy laws. In bulk material there are typically two main scattering mechanisms i.e. the acoustic or optical phonon scattering and the collision on neutral or charged impurities. For acoustic phonon lattice scattering, the mobility energy function reads (3,9),

$$\mu_{ac}(E,T) = \frac{q\pi\rho u_s^2\hbar^4}{\sqrt{2}E_1^2 m^{*5/2}T}\frac{1}{E^{1/2}} \tag{4}$$

where u_s is the sound velocity ($\simeq 10^5$ cm/s), ρ is the specific mass density (2 to 4 g/cm^3), E_1 is the acoustic deformation potential (5 to 8 eV), T is the temperature, and $\hbar$ is the reduced Planck constant. For optical phonon scattering more

complicated expressions have been worked out such as (3,10).

$$\mu_{\text{op}}(E,T) = \frac{4q\pi\rho\hbar^2 k\theta}{2^{3/2}m^{*5/2}D_0^2}\frac{1}{(n_0+1)(E-k\theta)^{1/2}n_0(E+k\theta)^{1/2}} \tag{5}$$

where $n_0 = 1/[\exp(\theta/T) - 1]$ is the phonon distribution function, θ is the optical phonon temperature, D_0 is a constant (≈ 4–6×10^8 eV/cm), and k is the Boltzmann constant.

For Coulomb or ionized impurity scattering the mobility is well described by the Brooks–Herring formula (11,12),

$$\mu_{\text{ii}}(E) = \frac{16\sqrt{2}\epsilon^2}{q^3\sqrt{m^*}N_{\text{i}}}\frac{E^{3/2}}{\ln(1+b) - \dfrac{b}{1+b}} \qquad \text{with} \qquad b = \frac{8m^*\lambda_{\text{s}}^2 E}{\hbar^2} \tag{6}$$

where N_{i} is the ionized impurity density, ϵ is the silicon dielectric permittivity, and λ_{s} is the screening length.

When several scattering processes play a role independently in the material, the Matthiessen rule stipulates that one can add separately the probability of each scattering rate for a given kinetic energy E such that the total mobility $\mu_{\text{tot}}(E)$ can be obtained, approximately, from

$$\frac{1}{\mu_{\text{tot}}(E)} = \frac{1}{\mu_{\text{ac}}(E)} + \frac{1}{\mu_{\text{ii}}(E)} + \cdots \tag{7}$$

For a nondegenerate semiconductor, the Boltzmann statistics apply so that the mean kinetic energy of the carriers is $\langle E\rangle = 3kT/2$. Therefore, the temperature dependence of the mobility can be approximately obtained by replacing E by $3kT/2$ in the scattering equations, yielding a $T^{-3/2}$ and $T^{3/2}$ theoretical dependence for acoustic phonon and ionized impurity scattering, respectively (3,4).

Another important transport coefficient directly related to the mobility is the so-called diffusion constant or diffusivity, D. This coefficient relates the diffusion current to the carrier concentration gradient as $\mathbf{J} = -\text{q}D\nabla\mathbf{n}$ (Fick's law). The equation between the mobility and the diffusivity is known as the (generalized) Einstein relation and is given by (3,4)

$$q^2 D = \frac{\sigma}{\partial n/\partial E_{\text{f}}} \tag{8}$$

This equation reduces to the classical Einstein relation for nondegenerate semiconductors as $qD = \mu_{\text{c}}kT$ for isotropic materials.

MOBILITY IN BULK SILICON AND GALLIUM ARSENIDE

The electron and hole mobility in semiconductors has been the subject of much research for many years (11,13–17). Most of the effort has been made to measure and interpret the mobility dependence with temperature and carrier concentration. Both the majority and minority carrier mobilities have been studied in order to provide reliable data and empirical laws applicable to device simulation. The majority carrier mobility prevails for devices such as junction field effect transistors (JFET) and accumulation-mode MOSFETs. The minority carrier mobility is mostly important for devices where carrier injection is dominant as in bipolar transistors and junction diodes. Therefore, in this section typical mobility data for bulk silicon and gallium arsenide materials are presented for majority and minority carrier transport.

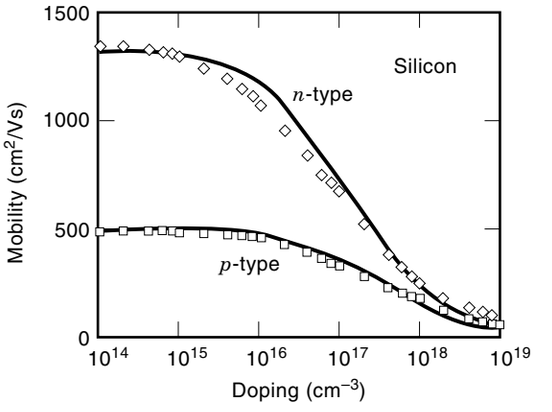

Figure 1. Experimental (symbols) and theoretical (solid lines) variations of the electron and hole mobility with doping concentration for bulk silicon [Data points from *ATLAS User Manual,* SILVACO Int., April 1997 (20)].

Bulk Silicon

The majority carrier mobility dependence with doping concentration is illustrated in Fig. 1 for bulk silicon as measured at room temperature. As it is clear from this figure, the electron and hole mobility does decrease as the doping level is increased, being divided by 2 for a concentration around $10^{17}/\text{cm}^3$. This typical behavior is well interpreted by a combination of phonon and ionized impurity scatterings as indicated by the solid lines in Fig. 1 obtained with the transport model of Eqs. (2)–(7). To this end only two parameters have been used to fit the data from low to high doping densities: the respective amplitude of acoustic phonon intensity and coupling constant for ionized impurity collision (9,10,18,19).

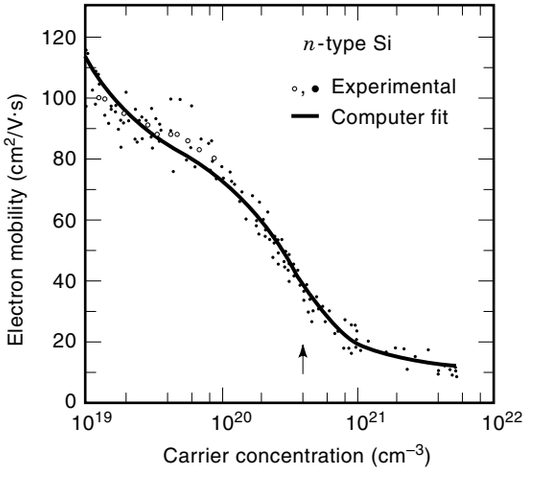

Figure 2. Experimental (symbols) and theoretical (solid line) variations of the electron mobility with doping concentration for bulk silicon; the fitting curves are obtained using Eq. (9) (After Masetti et al. *IEEE Trans. Electron. Devices,* **ED-30**: 767, 1983).

For higher doping concentration a deviation from the simple model valid up to $10^{19}/cm^3$ does appear, which can be well explained by the incomplete ionization rate of impurities and additional scattering term by neutral impurities (9,10,18,19). Empirical models have been proposed to fit Si mobility data from low to very high doping concentrations (9,10,18,19,21). A simple formula for the electron mobility is given by (17,19),

$$\mu_n = \mu_{min} + \frac{\mu_{max} - \mu_{min}}{1 + (N/C_r)^{\alpha}} - \frac{\mu_1}{1 + (C_s/N)^{\beta}} \tag{9}$$

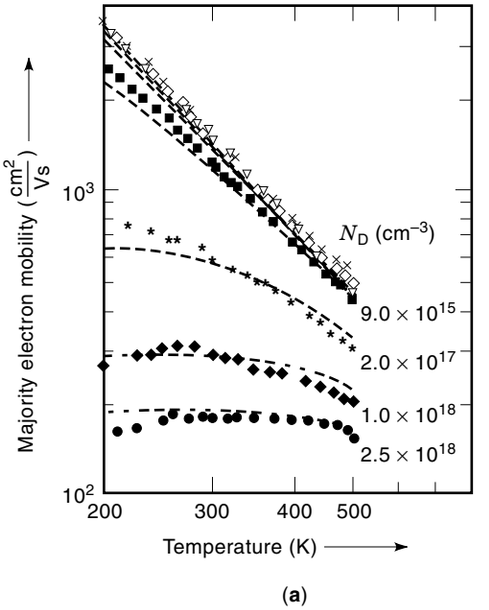

(a)

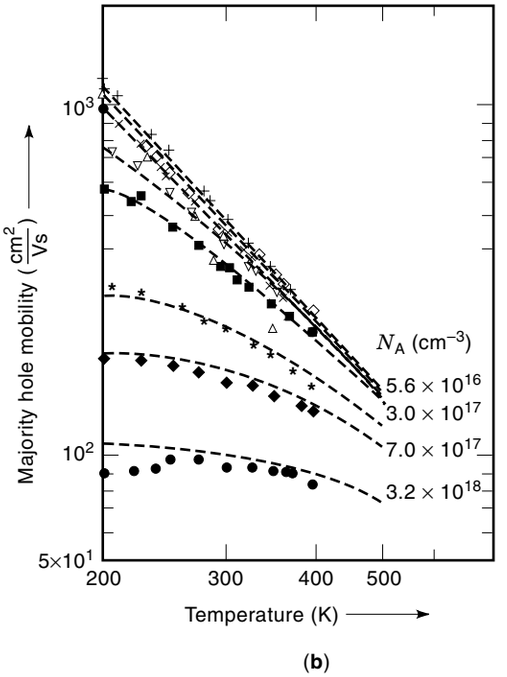

(b)

Figure 3. Experimental (symbols) and theoretical (dashed lines) variations of the electron (a) and hole (b) mobility with temperature for various doping concentrations in silicon (After Klaasen, *Solid State Electron.,* **35**: 961, 1992).

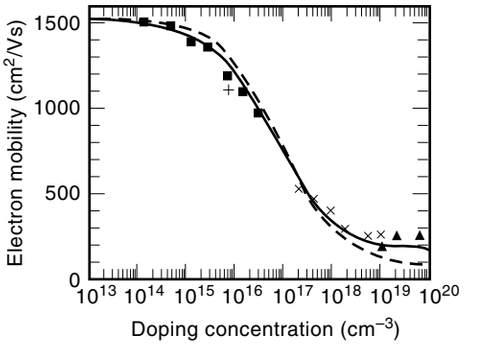

(a)

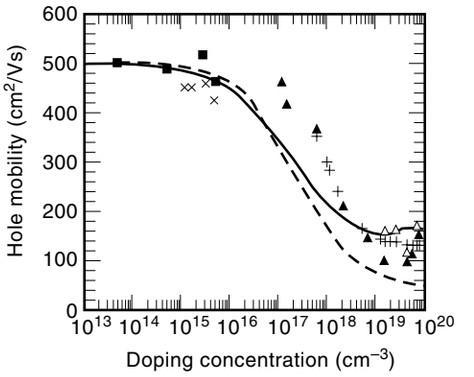

(b)

Figure 4. Experimental (symbols) and theoretical (solid lines) variations of electron (a) and hole (b) minority carrier mobility with doping concentration in bulk silicon. The dashed lines show the corresponding curves for the majority carrier mobilities. All theoretical curves are calculated with Klaassen's model (21) (After Stephens and Green, *J. Appl. Phys.,* **74**: 6212, 1993).

where μ_{min} = 40 to 60 cm^2/Vs, μ_{max} = 1400 cm^2/Vs (470 cm^2/Vs for hole), μ_1 = 30–50 cm^2/Vs, $C_r \approx 10^{17}/cm^3$, $C_s \approx 3$ to $5 \times 10^{20}/cm^3$, $\alpha = 0.7$, and $\beta = 2$. Figure 2 shows typical fitting for electron mobility data obtained by using Eq. (9) for the doping range $10^{19}/cm^3$ to $10^{22}/cm^3$.

The temperature variation of the majority carrier mobility has been discussed in terms of acoustic phonon and Coulomb scattering since the early 1950s (11,13). Representative electron and hole mobility data versus temperature are displayed in Fig. 3 for various donor and acceptor doping levels. The mobility decreases with T^{-2} for low doping density and is characteristic of a phonon scattering process. The flattening or small increase of the mobility with temperature is due to the increased contribution of the ionized impurity scattering at higher doping concentration. Empirical mobility models have been proposed to fit these temperature variations (dashed lines of Fig. 3) (9,22).

The mobility of minority carriers is a key parameter, for example, in bipolar transistors since it controls the transit time across the base. For this reason, a lot of studies has been devoted to its measurements and modeling (21,23–26). Both photo-injection (27) or electrical injection (26) techniques have been used for its assessment. Figure 4 shows typical variation of the minority carrier mobility for electrons and holes as

measured by microwave reflectance photo-injection technique (27). It is worth noting from this figure that the minority mobility is not very much different from the majority one. This feature has been well interpreted on the basis of the electron-hole scattering process (21,23). Actually, early work by Fletcher (23) shows that the minority carrier mobility can be evaluated after considering that majority carriers act as charged impurity scatterers and vice versa. Therefore the minority carrier mobility can be approximately calculated using the same formula as for majority carriers after replacing the ionized impurity density N_i by $(n + p)$ (19) or $\sqrt{np}$ (24) (n and p referring to the free electron and hole concentration, respectively).

Gallium Arsenide

The majority and minority carrier mobility dependence with doping concentration measured at room temperature for bulk GaAs is displayed in Fig. 5 (a–c). As for silicon, the carrier mobility follows the same behavior with a maximum value of about 7000 cm^2/Vs to 8000 cm^2/Vs reached at low doping where ionized impurity scattering is small and then decreases with the doping concentration. Note the very poor hole mobility amplitude which is close to that of silicon. The interpretation of such mobility data has been achieved with models similar to those used for bulk silicon including lattice and ionized impurity scattering for both majority and minority transport (16,17,28,29).

The temperature dependence of the electron and hole mobility in bulk GaAs has been studied intensively using Hall effect. Typical Hall mobility data are shown in Fig. 6 for various doping concentrations. As for bulk silicon the mobility decreases with $T^{-2.3}$ for low doping density due to prevailing polar phonon scattering and increases with $T^{1.5}$ at low temperature where ionized impurity scattering dominates (16,17).

For more information about the electrical properties of GaAs the reader should also refer to the article on III–V semiconductors.

MOBILITY IN FIELD EFFECT DEVICES

The transport in field effect devices has been intensively studied since the development of silicon MOSFETs in the 1960s and GaAs HFETs during the 1970s [see the extensive review by Ando et al. (30)]. The tremendous performance of Si MOSFETs leads to the progress of silicon microelectronics for the

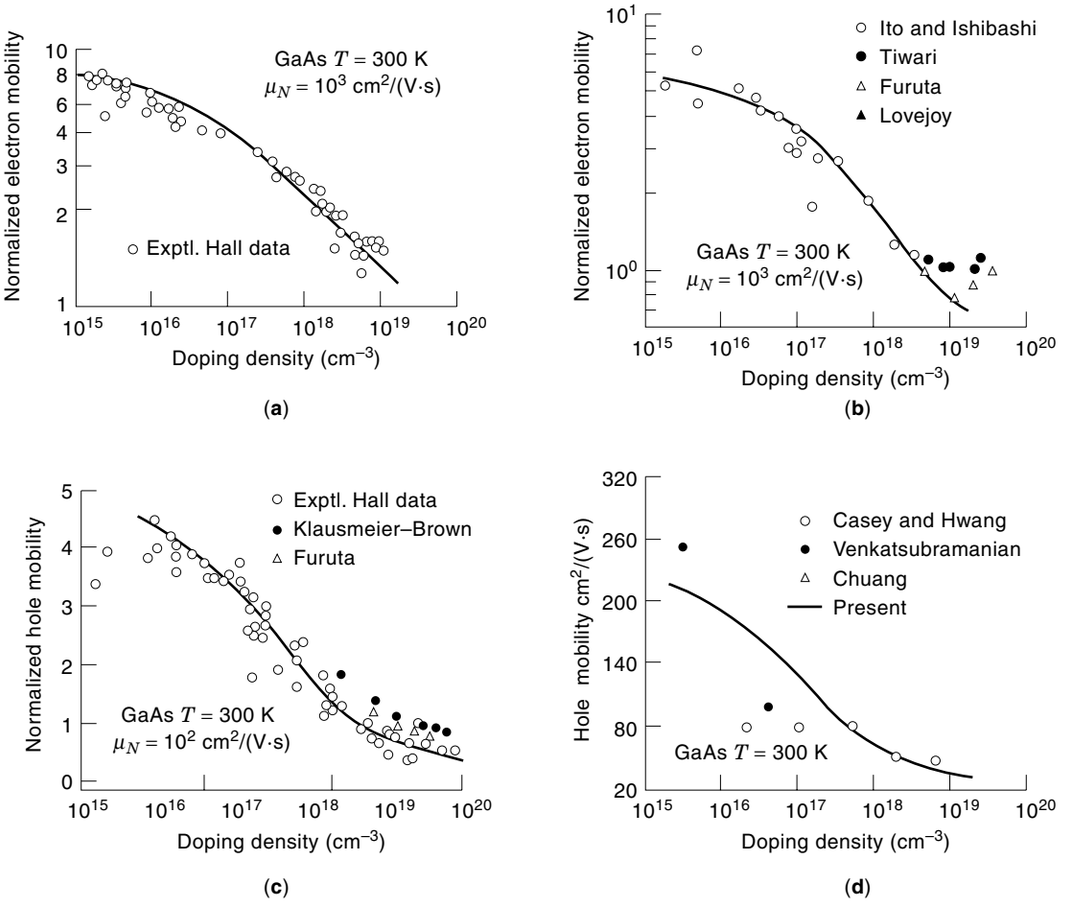

Figure 5. Experimental (symbols from various sources) and theoretical (solid lines) variations of majority electron (a), minority electron (b), majority hole (c), and minority hole (d) mobility with doping density in bulk GaAs (After S. N. Mohammad et al. *Solid State Electron.,* **36**: 1677, 1993).

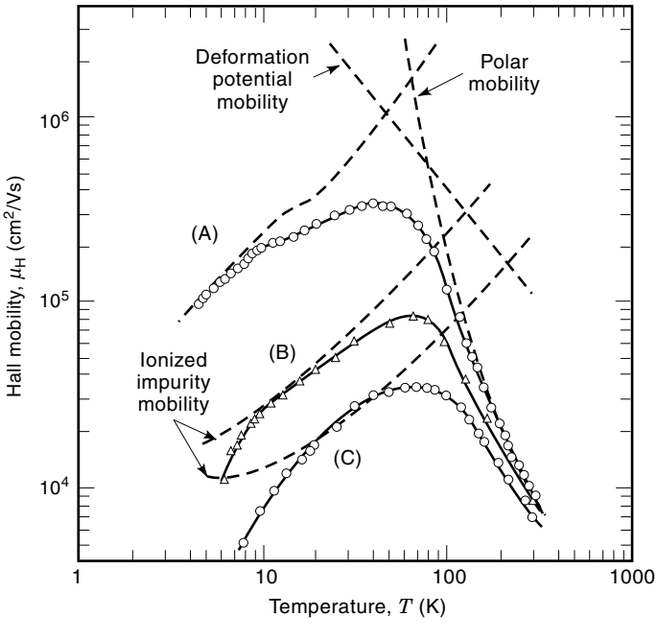

Figure 6. Experimental (symbols) and theoretical (dashed lines) variations of the electron Hall mobility with temperature for various doping density (A, 5×10^{13}/cm^3; B, 10^{15}/cm^3; and C, 5×10^{15}/cm^3) in bulk GaAs. The dashed line curves show the expected contributions of three major scattering processes (After Blakemore, *J. Appl. Phys.,* **53**: R123, 1982).

last 2 decades. This is due to the remarkable property of thermally grown silicon dioxide which allows a very good interface to be realized on silicon substrate. The high quality of SiO_2 leads to the excellent performance of Si MOSFETs in terms of gate dielectric isolation and channel-to-gate leakage current. Gallium arsenide does not benefit from such a nice gate dielectric, but newly developed deposition techniques such as molecular beam epitaxy (MBE) have been used to fabricate HFETs. The possibility of bandgap engineering based on AlGaAs alloy has enabled the carrier confinement in a nearly two-dimensional layer at the heterostructure interface. These HFETs have demonstrated much better transport properties as compared to bulk GaAs Metal Semiconductor Field-Effect Transistors (MESFETs).

Mobility in Si MOSFETs

The mobility in silicon inversion layers of MOSFETs has been the subject of much research during the last decades (30–36). The inversion layer carriers are localized within a few nanometers from the Si–SiO_2 interface and thus are subject to an additional scattering process related to the interface roughness. This gives rise to peculiar mobility behavior as compared to bulk silicon. The confined character of the inversion layer also leads to the energy quantification in the direction perpendicular to the interface forming two-dimensional (2-D) energy subbands (30). An important parameter for such 2-D systems is the effective electric field within the inversion layer defined as (30)

$$E_{\text{eff}} = \frac{\eta Q_{\text{i}} + Q_{\text{d}}}{\epsilon} \tag{10}$$

where Q_{i} is the inversion charge, Q_{d} is the depletion charge, and η is a weighting factor close to 1/2.

The carrier scattering in MOSFET inversion layers is basically governed by similar mechanisms as in bulk material: that is, phonon and charged impurity scattering processes to which one might add the surface roughness scattering due to the interface asperity. The theory of phonon scattering in 2D systems predicts a mobility behavior with T^{-1} (like in bulk silicon) and $E_{\text{eff}}^{-1/3}$ due to the limited extension of the inversion layer (37). The scattering by charged impurities located close to the inversion layer leads to a mobility varying with T (instead of $T^{3/2}$ for bulk material) and as N_{i}^{-1} (the areal ionized impurity density) (38). Surface roughness scattering yields a reduction of the mobility with E_{eff}^{-2} and $(\Delta L)^{-2}$ with the mean asperity, Δ, and length, L, of the surface roughness (39). As for bulk transport the overall mobility can be evaluated after adding the different scattering rates using the Matthiessen rule.

Typical variations of the mobility in Si MOSFETs which illustrate its universal dependence with effective electric field E_{eff} are given in Fig. 7. At low field the mobility reaches a plateau whose level depends primarily on the substrate doping density in the bulk material. This typical mobility behavior has lead to an empirical law, useful for Si MOSFET device simulation, of the form (32,40,41)

$$\frac{1}{\mu_{\text{eff}}} = \frac{1}{\mu_0} + a_1 E_{\text{eff}}^1 + a_2 E_{\text{eff}}^2 + \cdots \tag{11}$$

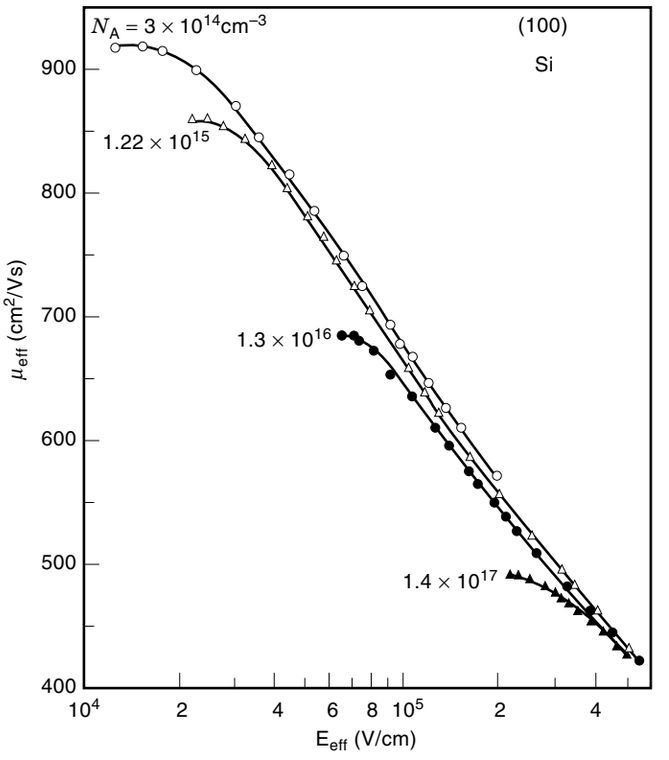

Figure 7. Experimental variations of inversion layer mobility with effective electric field, E_{eff}, for room temperature in silicon MOSFETs for various substrate doping concentrations (After Sun and Plummer, *IEEE Trans. Electron Devices,* **ED-27**: 1497, 1998).

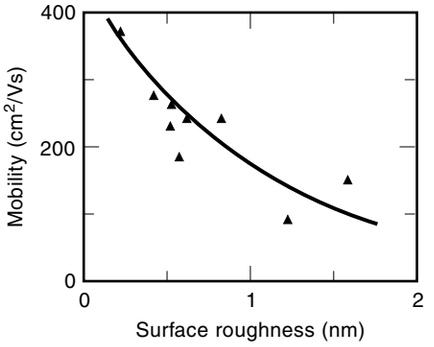

Figure 8. Experimental (symbols) and theoretical (solid line) variations of the effective mobility with the surface roughness in Si MOSFETs (After Rais et al., *Phys. Status Solidi A,* **146**: 853, 1994).

where μ_0 is the zero field mobility, and $a_{1,2}$ are constant parameters. The zero field mobility is close to that of bulk silicon for the given doping density (see Fig. 1).

The correlation between the surface roughness and the MOSFET mobility has been studied experimentally based on Scanning Tunneling Microscopy (STM) or Atomic Force Microscopy (AFM) measurements (42,43). Figure 8 shows that the mobility dependence with mean roughness can be well interpreted by a model in which the local mobility is gradually reduced to zero as the carriers are placed closer to the interface (41).

The temperature dependence of the transport in MOSFET inversion layers can be evaluated as in bulk material using the Kubo–Greenwood formulation of Eq. (2). Figure 9 gives typical behavior of MOSFET mobility with inversion charge as obtained for various temperatures. The modeling of these variations has been achieved by considering a bell-shaped energy mobility function $\mu(E)$ which embodies the Coulomb and surface roughness scattering (35). At very low temperature where the inversion layer is degenerate, the mobility reduces to $\mu(E_f)$. Since in 2-D systems the density of states is constant, E_f is proportional to the inversion charge, which justifies the bell-shaped curve for the mobility with Q_i (35). This bell-shaped behavior of the mobility with inversion charge has been successfully used to develop mobility models valid from 4 K up to 300 K, allowing the modeling of the MOSFET transfer characteristics over a wide temperature range (45).

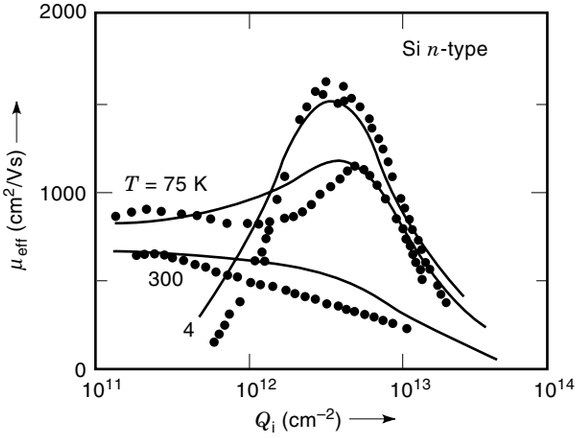

Figure 9. Experimental (symbols) and theoretical (solid lines) variations of inversion layer electron mobility with inversion charge density, Q_i, for various temperatures as obtained in silicon MOSFETs (44).

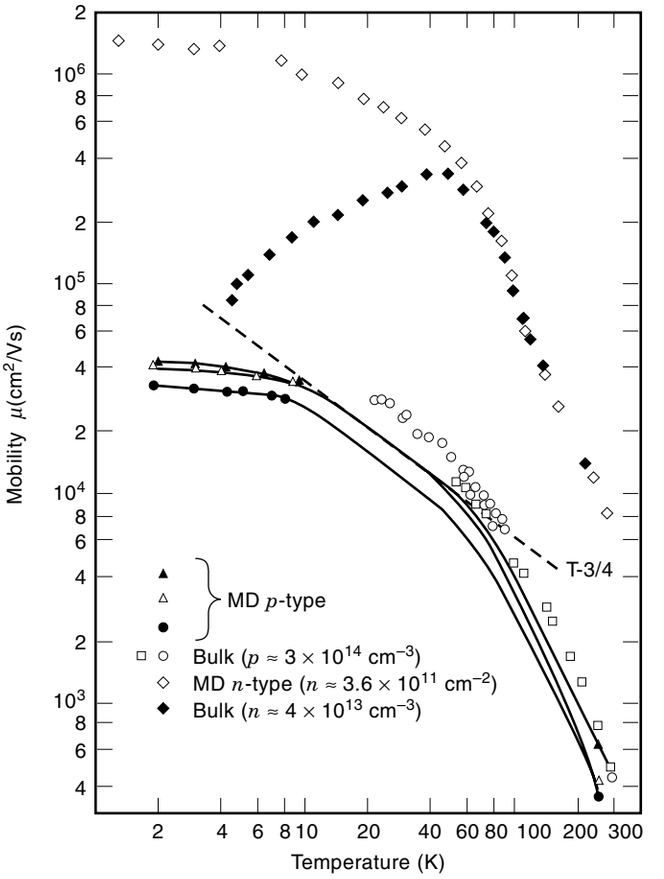

Figure 10. Temperature dependence of hole and electron mobility in GaAs HFETs and bulk GaAs for various structures (After Stormer et al., *Appl. Phys. Lett.,* **44**: 139, 1984).

Mobility in GaAs HFETs

The transport properties of GaAs HFETs are partly controlled by the same mechanisms that limit the carrier mobility in silicon inversion layers (30). The main difference resides in the polar nature of most heterostructure materials which enhances phonon scattering. The remarkable transport properties of GaAs HFETs arise essentially from the huge reduction of Coulomb scattering owing to the separation of the AlGaAs carrier supply layer from the 2-D channel (46–48). This is made possible by the modulation doping of AlGaAs layer while keeping the GaAs channel film undoped. This way the carriers in the channel at the AlGaAs/GaAs interface can move in a region almost free of charged impurities. Further improvement to the mobility can be obtained after introducing an undoped spacer region in the AlGaAs film close to the channel. As a result the scattering by remote ionized impurities can be significantly reduced for 10 nm to 20 nm thick spacer layers (46,47).

The temperature dependence of the mobility in GaAs HFETs resembles that for bulk material. Typical variations of the mobility with temperature are shown in Fig. 10 for electrons and holes in various modulation doped (MD) GaAs HFETs (49). Note that the electron mobility exceeds several millions at very low temperatures due to the extinction of phonon scattering and the quasi suppression of Coulomb scattering as compared to that of lightly doped bulk GaAs. The T^{-2} dependence of the mobility both for electrons and holes above 77 K is well explained by polar phonon scattering, as in bulk GaAs.

The variation of mobility with the 2-D carrier concentration in GaAs HFETs shows similar trends as that of silicon inversion layers (30,47,48,50,51). At room temperature the mobility is rather constant or slightly decreasing with carrier concentration (48). At very low temperature, as in inversion layer the mobility does increase with 2-D carrier density as illustrated in Fig. 11. This feature can be understood as in Fig. 9 by ionized impurity scattering in degenerate 2-D subbands (50).

The influence of undoped AlGaAs spacer on the Hall mobility in HFETs is illustrated in Fig. 12 (52). The reduction of impurity scattering at low temperature can be well interpreted by the theory of remote Coulomb scattering (53,54). This feature clearly demonstrates the impact of the material deposition technique on device performance.

Conventional GaAs HFETs have successfully been replaced by pseudomorphic AlGaAs/GaInAs MD structures where the band discontinuity at the channel interface has been increased allowing better carrier confinement at high gate voltages with good mobilities (48). This leads to higher current drive capability and in turn to larger operating frequencies.

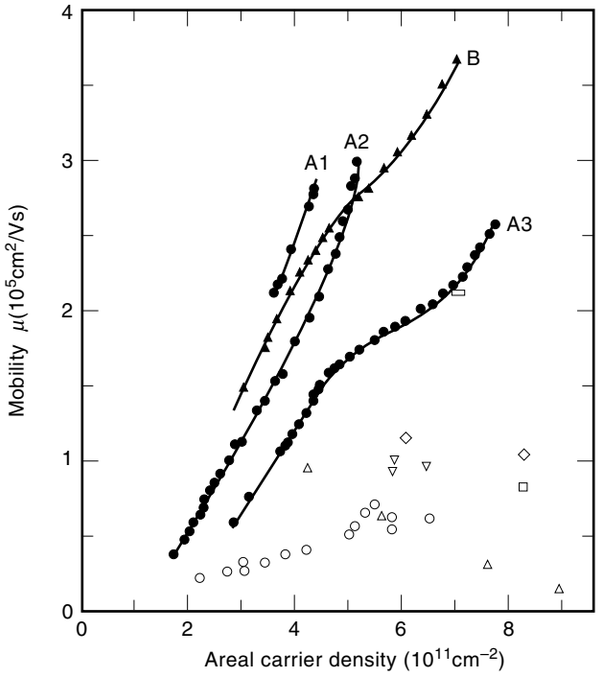

Figure 11. 2-D carrier density dependence of the mobility of various GaAs HFETs measured at liquid helium temperature (After Stormer et al., *Appl. Phys. Lett.,* **39**: 1981).

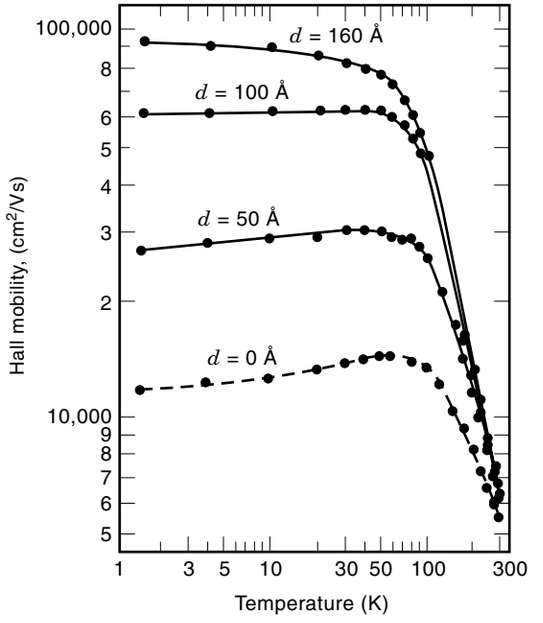

Figure 12. Influence of undoped spacer thickness d on the temperature dependence of the Hall mobility in GaAs HFETs (After Stormer et al., *Appl. Phys. Lett.,* **38**: 691, 1981).

BIBLIOGRAPHY

1. F. M. Bufler, et al., Low- and high-field electron transport parameters for unstrained and strained $Si_{1-x}Ge_x$, *IEEE Electron Device Lett.,* **EDL-18**: 264–266, 1996.
2. P. Bouillon, et al., *Proc. IEEE Int. Electron Device Meet.* IEDM96, Tech. Dig., 1996, pp. 559–563.
3. B. R. Nag, *Theory of Electrical Transport in Semiconductors,* Oxford: Pergamon, 1972.
4. J. Dugdale, *The Electrical Properties of Metals and Alloys,* London: Arnold, 1977.
5. M. Mott and E. Davis, *Electronic Proceses in Non-Crystalline Materials,* Oxford: Clarendon, 1979.
6. G. Ghibaudo, A simple derivation of the Kubo-Greenwood formula, *Phys. Status Solidi B,* **153**: K155–K158, 1989.
7. G. Ghibaudo, Analysis of the Hall effect in the localized states below the mobility edge, *J. Phys. C, Solid State Phys.,* **20**: L769–L773, 1987.
8. W. C. Mitchel and P. M. Hemenger, Temperature dependence of the Hall factor and the conductivity mobility in *p*-type silicon, *J. Appl. Phys.,* **53**: 6880–6884, 1982.
9. S. Li, The dopant density and temperature dependence of hole mobility and resistivity in boron doped silicon, *Solid State Electron.,* **21**: 1109–1117, 1978.
10. S. Li and W. R. Thurber, The dopant density and temperature dependence of electron mobility and resistivity in *n*-type silicon, *Solid State Electron.,* **20**: 609–616, 1977.
11. H. Brooks, Theory of electrical properties of germanium and silicon, in L. Marton (ed.), *Advances Electronics and Electron Physics,* New York: Academic Press, 1955, vol. 7, pp. 85–182.

12. D. Chattopadhyay and H. J. Queisser, Electron scattering by ionized impurities in semiconductors, *Rev. Mod. Phys.,* **53**: 745–768, 1981.
13. F. J. Morin and J. P. Maita, Electrical properties of silicon containing arsenic and boron, *Phys. Rev.,* **96**: 28–35, 1954.
14. D. Long, Scattering of conduction electrons by lattice vibrations in silicon, *Phys. Rev.,* **120**: 2026–2032, 1960.
15. D. M. Caughey and R. E. Thomas, Carrier mobility in silicon empirically related to doping and field, *Proc. IEEE,* **55**: 2192–2193, 1967.
16. J. S. Blakemore, Semiconducting and other major properties of gallium arsenide, *J. Appl. Phys.,* **53**: R123–R180, 1982.
17. J. D. Wiley, Willardson and Beer (eds.), in *Semiconductors and Semimetals,* vol. 10, New York: Academic Press, 1974, p. 91.
18. N. Arora, J. R. Hauser, and D. J. Roulston, Electron and hole mobilities in silicon as a function of concentration and temperature, *IEEE Trans. Electron Devices,* **ED-29**: 292–295, 1982.
19. G. Masetti, M. Severi, and S. Solmi, Modeling of carrier mobility against carrier concentration in arsenic-, phosphorus-, and boron-doped silicon, *IEEE Trans. Electron Devices,* **ED-30**: 767–769, 1983.
20. *ATLAS User Manual,* Device simulation software from SILVACO International, Santa Clara, CA, Version 1.5.0, April 1997, p. 3.11.
21. D. B. M. Klaassen, A unified mobility model for device simulation-I. Model equations and concentration dependence, *Solid State Electron.,* **35**: 953–959, 1992.
22. D. B. M. Klaassen, A unified mobility model for device simulation-II. Temperature dependence of carrier mobility and lifetime, *Solid State Electron.,* **35**: 961–967, 1992.
23. N. Fletcher, The high current limit for semiconductor junction devices, *Proc. IRE,* 862–872, 1957.
24. J. Dorkel and P. Leturck, Carrier mobilities in silicon semi-empirically related to temperature, doping and injection level, *Solid State Electron.,* **24**: 821–825, 1981.
25. V. Grivtiskas, M. Willander, and J. Vaitkus, The role of intercarrier scattering in excited silicon, *Solid State Electron.,* **27**: 565–572, 1984.
26. S. Bellone, G. V. Persiano, and A. G. Strollo, Electrical measurement of electron and hole mobilities as function of injection level in silicon, *IEEE Trans. Electron Devices,* **ED-43**: 1459–1465, 1996.
27. A. W. Stephens and M. A. Green, Minority carrier mobility of Czochralski-grown silicon by microwave-detected photoconductance decay, *J. Appl. Phys.,* **74**: 6212–6216, 1993.
28. J. R. Lowney and H. S. Bennet, Majority and minority electron and hole mobilities in heavily doped GaAs, *J. Appl. Phys.,* **69**: 7102–7110, 1991.
29. S. N. Mohammad et al., Temperature, electric field, and doping dependent mobilities of electrons and holes in semiconductors, *Solid State Electron.,* **36**: 1677–1683, 1993.
30. T. Ando, A. B. Fowler, and F. Stern, Electronic properties of two-dimensional systems, *Rev. Mod. Phys.,* **54**: 437–630, 1982.
31. F. F. Fang and A. B. Fowler, Transport properties of electrons in inverted silicon surfaces, *Phys. Rev.,* **169**: 619–631, 1968.
32. A. G. Sabnis and J. T. Clemens, Characterization of the electron mobility in the inverted ⟨100⟩ Si surface, *Tech. Digest IEDM,* 18–21, 1979.
33. S. C. Sun and J. D. Plummer, Electron mobility in inversion and accumulation layers on thermally oxidized silicon surfaces, *IEEE Trans. Electron Devices,* **ED-27**: 1497–1508, 1980.
34. H. Shin et al., Physically-based models for effecive mobility and local-field mobility of electrons in MOS inversion layers, *Solid State Electron.,* **34**: 545–552, 1991.
35. G. Ghibaudo, Transport in the inversion layer of a MOS transistor: Use of Kubo-Greenwood formalism, *J. Phys. C: Solid State Phys.,* **19**: 767–777, 1985.
36. F. Gamiz et al., Universality of electron mobility curves in MOSFETs: A Monte Carlo study, *IEEE Trans. Electron Devices,* **ED-42**: 258–264, 1995.
37. S. Kawaji, The two-dimensional lattice scattering mobility in a semiconductor inversion layer, *J. Phys. Soc. Jpn.,* **27**: 906–908, 1969.
38. C. T. Sah, T. H. Ning, and L. L. Tschopp, The scattering of electrons by surface oxide charges and by lattice vibrations at the silicon-silicon dioxide interface, *Surf. Sci.,* **32**: 561–575, 1972.
39. A. Harstein, T. H. Ning, and A. B. Fowler, Electron scattering in silicon inversion layers by oxide and surface roughness, **58**: 178–181, 1976.
40. M.-S. Lin, A better understanding of the channel mobility of Si MOSFETs based on the physics of quantized subbands, *IEEE Trans. Electron Devices,* **ED-35**: 2406–2411, 1988.
41. K. Rais, G. Ghibaudo, and F. Balestra, Surface roughness mobility model for silicon MOS transistors, *Phys. Status Solidi A,* **146**: 853–858, 1994.
42. T. Ohmi et al., Dependence of electron channel mobility on $Si\text{-}SiO_2$ interface microroughness, *IEEE Electron Device Lett.,* **EDL-12**: 652–654, 1991.
43. T. Yamanaka et al., Correlation between inversion layer mobility and surface roughness measured by AFM, *IEEE Electron Device Lett.,* **17**: 178–180, 1996.
44. G. Ghibaudo, An analytical model of conductance and transconductance for enhanced mode MOSFETs, *Phys. Status Solidi A,* **95**: 323–335, 1986.
45. A. Emrani, F. Balestra, and G. Ghibaudo, Generalized mobility law for drain current modeling in Si MOS transistors from liquid helium to room temperatures, *IEEE Trans. Electron Devices,* **ED-40**: 564–570,1993.
46. M. Shur, *GaAs Devices and Circuits,* New York: Plenum, 1987.
47. S. J. Pearton and N. J. Shah, Heterostructure field effect transistors, in *High-Speed Semiconductor Devices,* New York: Wiley, 1990.
48. L. D. Nguyen, L. E. Larson, and U. K. Mishra, Ultra-high speed modulation doped field effect transistors: A tutorial review, *Proc. IEEE,* **80**: 494–518, 1992.
49. H. L. Stormer et al., Temperature dependence of the mobility of two-dimensional hole systems in modulation-doped GaAs-(AlGa)As, *Appl. Phys. Lett.,* **44**: 139–141, 1984.
50. H. L. Stormer et al., Dependence of electron mobility in modulation-doped GaAs-(AlGa)As heterojunction interfaces on electron density and Al concentration, *Appl. Phys. Lett.,* **39**: 912–914, 1981.
51. T. J. Drummond et al., Electron mobility in single and multiple period modulation-doped (Al,Ga)As/GaAs heterostructures, *J. Appl. Phys.,* **53**: 1023–1027, 1982.
52. H. L. Stormer et al., Influence of an undoped (AlGa)As spacer as mobility enhancement in GaAs-(AlGa)As superlattices, *Appl. Phys. Lett.,* **38**: 692–693, 1981.
53. A. A. Grinberg and M. S. Shur, Effect of image charges on impurity scattering of two-dimensional electron gas in AlGaAs/GaAs, *J. Appl. Phys.,* **58**: 382–386, 1985.
54. J. Lee, H. N. Spector, and V. Arora, Quantum transport in a single layered structure for impurity scattering, *Appl. Phys. Lett.,* **42**: 363–365, 1983.

GÉRARD GHIBAUDO
UMR CNRS, ENSERG